PD+SMC Quadrotor Control for Altitude and Crack Recognition Using Deep Learning

J. Vazquez-Nicolas, Erik Zamora, Iván González-Hernández, Rogelio Lozano, Humberto Sossa

▶ **To cite this version:**

J. Vazquez-Nicolas, Erik Zamora, Iván González-Hernández, Rogelio Lozano, Humberto Sossa. PD+SMC Quadrotor Control for Altitude and Crack Recognition Using Deep Learning. International Journal of Control, Automation and Systems, 2020, 18 (4), pp.834-844. 10.1007/s12555-018-0852-9 . hal-03782873

HAL Id: hal-03782873
https://hal.science/hal-03782873

Submitted on 23 Nov 2023

HAL is a multi-disciplinary open access archive for the deposit and dissemination of scientific research documents, whether they are published or not. The documents may come from teaching and research institutions in France or abroad, or from public or private research centers.

L'archive ouverte pluridisciplinaire **HAL**, est destinée au dépôt et à la diffusion de documents scientifiques de niveau recherche, publiés ou non, émanant des établissements d'enseignement et de recherche français ou étrangers, des laboratoires publics ou privés.

PD+SMC Quadrotor Control for Altitude and Crack Recognition Using Deep Learning

J. M. Vazquez-Nicolas*, Erik Zamora, Iván González-Hernández, Rogelio Lozano, and Humberto Sossa

Abstract: Building inspection is a vital task because infrastructure damage puts people at risk or causes economic losses. Thanks to the technological breakthroughs in regard to Unmanned Aerial Vehicles (UAVs) and intelligent systems, there is a real possibility to implement an inspection by means of these technologies. UAVs allow reaching difficult places and, depending on the hardware carried onboard, take data or compute algorithms to understand the environment. This paper proposes a real-time robust altitude control strategy for a quadrotor aircraft, also a convolutional neuronal network for crack recognition is developed. The main idea of this proposal is to lay the background for an autonomous system for the inspection of structures using a UAV. For the robust control, a combination of two control actions, one linear (PD) and another nonlinear (Sliding Mode) is used. The combination of these control actions allows increasing the system's performance. To verify the satisfactory performance of proposed control law, simulations and experimental results with a quadrotor, in the presence of disturbances, are presented. For crack recognition in images, several experiments were carried out validating the proposed model. For CNN training, a database of cracks was built from images taken from the Internet.

Keywords: Deep learning, embedded control system, inspection, quadrotor aircraft, robust altitude control, UAV.

1. INTRODUCTION

Unmanned aerial vehicles (UAVs) have become a helpful tool for performing autonomous tasks in the industrial, commercial and research areas. Given your advantages (managed remotely or autonomously, fly over areas of difficult access, etc.), these robots are an ideal tool for inspection, as the case of structures. In Mexico, as well as in other parts of the world, natural disasters are frequent. On September 19, 2017, the worst earthquake in the story of Mexico, since 1985, was occurred. Many buildings suffered structural damages (see Fig. 1) which put the lives of people at risk.

The need to inspect buildings became evident during this tragic event. The civil protection protocol indicates that an inspector must return to the building and identify the risks of the structure and, if there are any, do not allow the re-entry to the building. In this sense, the inspector runs a risk when re-entering the building to perform the inspection. The difficulty of carrying out the check is that the areas to be inspected are usually difficult to access or there exist a risk for the human inspector. One of the most common failures are cracks, which can put at risk the structure and the integrity of people.

To improve the previous work [1] where a Convolutional Neural Network (CNN) was proposed to detect cracks in images taken by a quadrotor aircraft, the present work is focused on the robust altitude control of the UAV, in presence of external disturbances, and in the increase of the images dataset to re-train the CNN and improve their performance. Our future aim is to build an UAV-based autonomous inspection system for structures such as buildings, tunnels, bridges, etc. However, in this paper, we focus on the control subsystem and the crack recognition subsystem.

The main contribution of this work is an altitude hybrid control for a system based on a quadrotor aircraft, focused towards an autonomous wall inspection in the pres-

Fig. 1. Damaged building during an earthquake in Mexico in 2017.

ence of disturbances. The hybrid control proposed is a Proportional-Derivative (PD) plus a Sliding Mode Control (SMC). Experimental and simulation results are presented. Another contribution is the application of the proposal introduced in [1] to a more extensive database. This database is formed, mainly, by images of buildings damaged after the earthquake in Mexico City in 2017.

The rest of the paper is organized as follows: The related work is presented in Section II. Mathematical model of the vehicle is provided in Section III. Section IV gives the robust control strategy. Section V presents the simulation results for PD+SMC control. Section VI gives the CNN design and implementation. The real-time results are shown in Section VII. Finally, Section VIII gives the conclusion.

2. RELATED WORK

Unmanned Aerial Vehicles (UAV) have been an important research topic in recent years. In particular, the quadrotor helicopter has been under the focus of extensive research due to their many advantages. The control of these systems was extensively covered in the literature; for instance, PD linear control [2–7] and SMC [8–13] have been commonly used to control quadrotor systems.

In this work a hybrid PD+SMC is used to carry out the altitude control. This approach has been used to control robotic arms and robot teleoperation ([14–17]) but, to the best of our knowledge, this approach has not been used for a quadrotor UAV.

There are works focused on crack detection in structures, some using computer vision algorithms. The images for the experiments are commonly recollected by humans, in a safe area or with the help of a robotic system. However, in recent years, UAVs have been used to obtain images for inspection tasks, mainly in structures that involve risk for the human or in areas where access is difficult.

Concerning the detection of cracks without UAVs, in [19] authors used the color characteristics via a detection algorithm and, based on this information, an estimate of the length of the cracks is made. In [20], the authors implement crack detection in images of asphalt, where features extraction is carried out by decision trees and classification is performed by k-nearest neighbors method and support vector machines (SVM). Authors in [21], use classic computer vision techniques like edge detection (Sobel filter) and thresholding (Otsu algorithm) to locate cracks.

In [22], [23], and [24], present images which are obtained by means of UAVs and subsequently the detection of cracks was performed. In [22], the authors use lasers to generate a 3D model of the surface to be inspected for the autonomous navigation system, and the detection of cracks is made by means of the histogram and adaptive thresholds. Authors in [23], use classifiers and features extraction to find flaws on a wind generator blade surface. A UAV is used to take pictures of a generator. In [24] a UAV for building inspection is proposed, implementing a basic edge detection algorithm.

Given that our work uses deep learning approach to accomplish the cracks recognition, it is important to mention works related to applications of UAVs and convolutional neural networks (CNN). In [30], [31], [32], [33] and [34] where CNN were used to face problems such as high voltage inspection, vehicular traffic tracking, recognition of gestures, and crack recognition on pavement. Authors in [29] presents a crack recognition algorithm in images taken by a UAV using a CNN. In terms of deep learning, our work uses a smaller CNN structure than presented in [29] and the database of cracks were taken from damaged buildings.

3. DYNAMIC MODEL FOR QUADROTOR AIRCRAFT

The mathematical model of the quadrotor aircraft is widely discussed in the literature ([26], [27] and [28]) where the vehicle is considered as a rigid body that unfolds in three dimensions, which is subject to a main force and three moments that will be formulated by means of the Euler-Lagrange equations. Fig. 2 shows a free-body diagram of the quadrotor aircraft.

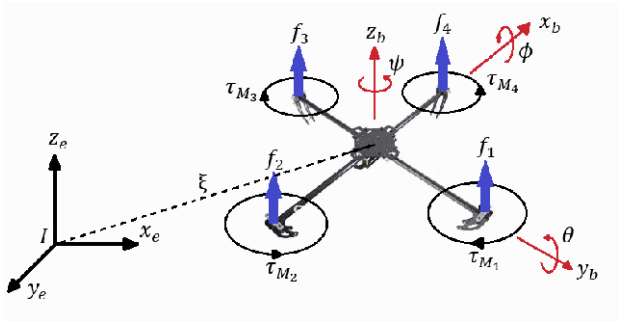

Fig. 2. Free-body diagram of the UAV.

The generalized coordinates of the vehicle are given by

$$q = (x, y, z, \psi, \theta, \phi) \in \mathbb{R}^6, \tag{1}$$

where we can define $\xi = (x, y, z) \in \mathbb{R}^3$ which denotes the position of the center of mass of the vehicle with respect to the inertial frame I and we also define $\eta = (\psi, \theta, \phi) \in \mathbb{R}^3$ which represents the angles of Euler, ψ is the angle of *yaw*, θ is the angle of *pitch* and ϕ is the angle of *roll* which are used to represent the orientation of the vehicle.

We can decompose the equations into translational and rotational displacement. As first step, we obtain the Lagrangian of the aerial vehicle, which is given by the following equation

$$L(q, \dot{q}) = T_{trans} + T_{rot} - U, \tag{2}$$

where $T_{trans} = \frac{m}{2}\dot{\xi}^T\dot{\xi}$, $T_{rot} = \frac{1}{2}\omega^T I\omega$ and $U = mgz$ are the translational kinetic energy, the rotational kinetic energy and the potential energy of the system, respectively. The Euler-Lagrange equation is used to obtain the quadrotor dynamic model

$$\frac{d}{dt}\frac{\partial \mathcal{L}}{\partial \dot{q}} - \frac{\partial \mathcal{L}}{\partial q} = \begin{bmatrix} F_\xi \\ \tau \end{bmatrix} = F, \tag{3}$$

where F_ξ is the translational force that is applied to the quadrotor and that is due to the control input that is a function of the force applied by the motors, $\tau \in \mathbb{R}^3$ refers to the moments of Euler's angles.

The translational force $F_\xi = R\hat{F}$ where R refers to the rotation matrix $R(\psi, \theta, \phi)$ of the vehicle with respect to a fixed reference axis.

We define the force $\hat{F} = [0\ 0\ u]^T$ and the control input $u = f_1 + f_2 + f_3 + f_4$ in such that

$$f_i = k_i \omega_i^2, \quad \forall i = 1, ..., 4, \tag{4}$$

where k_i is the value constant of the *i-st* engine and ω_i is its angular velocity. On the other hand, the moments are defined by:

$$\tau = \begin{bmatrix} \tau_\psi \\ \tau_\theta \\ \tau_\phi \end{bmatrix} \triangleq \begin{bmatrix} \sum_{i=1}^4 \tau_{M_i} \\ (f_2 - f_4)l \\ (f_3 - f_1)l \end{bmatrix}, \tag{5}$$

where l is the distance between the engines and the center of gravity of the vehicle, while τ_{M_i} represents the moment produced by the engine M_i, $i = 1, ..., 4$ around the center of gravity of the quadrotor aircraft.

Defining $C(\eta, \dot{\eta})$ as a function that represents the associated Coriolis terms to the gyroscopic and centrifugal effects corresponding to η

$$C(\eta, \dot{\eta}) = \dot{\mathbb{J}} - \frac{1}{2}\frac{\partial}{\partial \eta}(\dot{\eta}^T \mathbb{J}). \tag{6}$$

We can write the equations of the system as

$$F_\xi = m\ddot{\xi} + mgE_z, \tag{7}$$

$$\mathbb{J}\ddot{\eta} = -C(\eta, \dot{\eta})\dot{\eta} + \tau. \tag{8}$$

Using a change of the input variables

$$\tau = C(\eta, \dot{\eta})\dot{\eta} + \mathbb{J}\tilde{\tau}, \tag{9}$$

where $\tilde{\tau} = [\tilde{\tau_\psi}, \tilde{\tau_\theta}, \tilde{\tau_\phi}]^T$ Finally we obtain the system equations given by

$$\begin{aligned} m\ddot{x} &= -u\sin\theta, \\ m\ddot{y} &= u\cos\theta\sin\phi, \\ m\ddot{z} &= u\cos\theta\cos\phi - mg, \\ \ddot{\phi} &= \tilde{\tau}_\phi, \\ \ddot{\theta} &= \tilde{\tau}_\theta, \\ \ddot{\psi} &= \tilde{\tau}_\psi. \end{aligned} \tag{10}$$

4. ALTITUDE CONTROL BASED ON PD+SMC ALGORITHM

A widespread method for altitude control in a quadrotor UAV is a typical PD controller, which is widely used due to their simplicity and acceptable performance. However, for a real-time application where there are disturbances such as wind gusts, it is necessary to use a nonlinear control which provides robustness [11, 28]. One well-known control method is the Sliding Mode Controller (SMC). Both PD and SMC control have strengths and weaknesses, these motivate the use of a combination of these techniques.

4.1. Control design

The design problem is to enforce the behavior of the states towards the desired trajectories which are known. The following procedure describes how to determine a control law for any of the dynamics of the quadrotor (x, y, z, ψ, θ or ϕ). In this paper, the control for the z dynamics has been obtaining. Denote the reference trajectories by $\dot{z}_d$ and z_d which is velocity and altitude desired, respectively. Afterwards, we define the tracking errors by $e_z = z - z_d$ and $\dot{e}_z = \dot{z} - \dot{z}_d$, where z_d is the desired altitude. Since altitude control concerns only the displacement in the z-axis can be considered the following model from (10)

$$\ddot{z} = \frac{1}{m}(u\cos(\phi)\cos(\theta) - mg). \tag{11}$$

To start, the control law u is proposed as follows:

$$u = \frac{m(r+g)}{\cos(\phi)\cos(\theta)} \tag{12}$$

with

$$r = \underbrace{-k_p\tanh(e_z) - k_d\tanh(\dot{e}_z)}_{u_1}\underbrace{-\rho\,\mathrm{sign}(s)}_{u_2}, \tag{13}$$

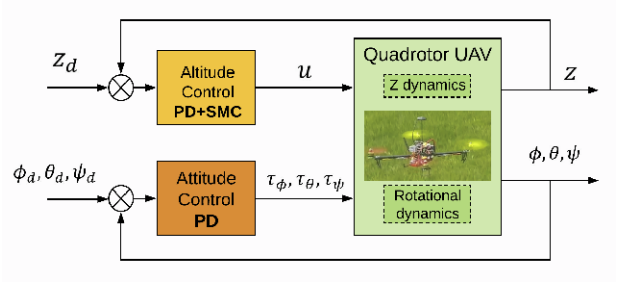

Fig. 3. Schematic of the control system.

where k_p, k_d and ρ are gains to tune the altitude controller while s is the sliding surface of SMC. In order to solve the input saturation problem, we use the approach used in [25], adding a tanh function to saturate the control input. A schematic of the control proposed is presented in Fig. 3.

Equation (13) has u_1 and u_2 that represents a PD and SMC control actions, respectively. The SMC control scheme introduces a "sliding surface" along which the sliding motion is to take place. This surface is denoted by s and is defined as follows:

$$\begin{aligned} s &= \left(\frac{d}{dt} + \lambda\right) e_z, \\ s &= \dot{e}_z + \lambda e_z, \end{aligned} \tag{14}$$

where $\lambda > 0$ is the slope of the sliding line. If a control law enforces the trajectories in the phase space such that $s = 0$ in (14), then the errors converge in a finite time to the origin due to

$$\begin{aligned} 0 &= \dot{e}_z + \lambda e_z, \\ \dot{e}_z &= -\lambda e_z, \end{aligned} \tag{15}$$

where the solution is: $e_z(t) = e_z(0)e^{-\lambda t}$. Consider the two-dimensional system [35]

$$\begin{aligned} \dot{x}_1 &= x_2, \\ \dot{x}_2 &= h(x) + p(x)u, \end{aligned} \tag{16}$$

where $h(x)$ and $p(x)$ are unknown locally Lipschitz functions and $p(x) \geq p_0$ for all x. The goal is to design a controller that constraints the trajectory to the manifold $s = ax_1 + x_2 = 0$. Choosing $a > 0$ guarantees that $x(t)$ tends to zero as t tends to infinity and the rate is controlled by the parameter a. The surface s satisfies the equation

$$\dot{s} = a\dot{x}_1 + \dot{x}_2 = ax_2 + h(x) + p(x)u. \tag{17}$$

Suppose that h and g satisfy

$$\left|\frac{ax_2 + h(x)}{p(x)}\right| \leq \rho(x), \quad \forall x \in \mathbb{R}^2. \tag{18}$$

This assumption allows us to define a bounded region by $\rho(x)$ to limit the control input of the SMC. Defining the states

$$x_1 = z \qquad x_2 = \dot{z}, \tag{19}$$

therefore

$$\dot{x}_1 = \dot{z} \qquad \dot{x}_2 = \ddot{z}, \tag{20}$$

so that our system is defined as

$$\dot{x}_1 = x_2, \tag{21}$$

$$\dot{x}_2 = \underbrace{-g}_{h(x)} + \underbrace{\left(\frac{\cos\phi\cos\theta}{m}\right)}_{p(x)} u, \tag{22}$$

under the restriction from (18)

$$\left|\frac{ax_2 + (-g)}{\frac{\cos\phi\cos\theta}{m}}\right| \leq \rho(x), \quad \forall x \in R^2, \tag{23}$$

where $\rho(x)$ is the upper bound of the states (altitude and velocity in the z-direction). For the design process, the control inputs (u_1 and u_2) are analyzed separately.

4.2. Stability analysis

We propose the following Lyapunov function candidate given as

$$V = \underbrace{\frac{1}{2}s^2}_{V_1} + \underbrace{\frac{1}{2}\dot{e}_z^2 + k_p \ln(\cosh(e_z))}_{V_2}. \tag{24}$$

The Lyapunov function candidate is composed by two parts: SMC control (V_1) and PD control (V_2) so the stability analysis is made separately.

4.2.1 Stability for V_1

For V_1 function, your derivative can be computed as follows:

$$\dot{V}_1 = s\dot{s}, \tag{25}$$

considering a control input $\tilde{u}$

$$\tilde{u} = -\beta(x)\,\mathrm{sign}(s), \tag{26}$$

thereby

$$\begin{aligned} \dot{V}_1 &\leq g(x)|s|\rho(x) - g(x)[\rho(x) + \beta_0]\,\mathrm{sign}(s)s \\ &\leq -g(x)\beta_0\,\mathrm{sign}(s)s, \end{aligned} \tag{27}$$

considering the next properties

$$\mathrm{sign}^{2n}(s) = 1 \quad \text{for} \quad n = 1, 2, 3\ldots, \tag{28}$$

$$s = \mathrm{sign}(s)\mathrm{abs}s \quad \text{for} \quad s \in \mathbb{R}, \tag{29}$$

we obtain

$$\begin{aligned} \dot{V}_1 &\leq -g(x)\beta_0|s| \\ &\leq -g_0\beta_0|s|, \end{aligned} \tag{30}$$

which implies that the system is asymptotically stable since $\dot{V}_1 < 0$ for $s \neq 0$ in the region bounded by $g_0\beta_0$.

4.2.2 Stability for V_2

The time derivative of V_2 is

$$\dot{V}_2 = \dot{e}_z \ddot{e}_z + k_p \tanh(e_z)\dot{e}_z, \tag{31}$$

where

$$\ddot{e}_z = \ddot{z} - \ddot{z}_d. \tag{32}$$

The goal to the control is to let $z_d = 0$ so $\ddot{e}_z = \ddot{z}$. From (11) and (13), we obtain

$$\begin{aligned}\dot{V}_2 =& \dot{e}_z(-k_p \tanh(e_z) - k_d \tanh(\dot{e}_z)) \\ &+ k_p \tanh(e_z)\dot{e} \\ =& -k_p \tanh(e_z)\dot{e} - k_d \dot{e} \tanh(\dot{e}_z) \\ &+ k_p \tanh(e_z)\dot{e} \\ =& -k_d \dot{e} \tanh(\dot{e}_z),\end{aligned} \tag{33}$$

which implies that the system is asymptotically stable since $\dot{V}_2 < 0$ for $\dot{e} \neq 0$.

5. SIMULATION RESULTS

Simulation results of the quad-rotor aircraft for altitude control (z-axis dynamic) are presented below. For simulation purposes, an external disturbance has been introduced to test the robustness of the control scheme proposed.

5.1. Wind-gust model

In order to perform a more realistic simulation of the system, wind effects are considered as disturbances. The wind model selected is the Dryden wind-gust. This model is defined as a sum of sinusoidal signals

$$v_\omega(t) = v_\omega^0 + \sum_{i=1}^{n} a_i \sin(\Omega_i t + \varphi_i), \tag{34}$$

where $v_\omega(t)$ is an estimate of the wind vector, Ω_i are randomly selected frequencies, φ_i are phase shifts, a_i is the amplitude of sinusoids and v_ω^0 is the static wind vector. The simulation was developed in the Simulink platform, where the force caused by the wind gust is considered proportional to the velocity given by (34). This force is shown in Fig. 4.

5.2. PD Control with Sliding Mode Compensation (PD+SMC)

Three different control laws were simulated; a) Proportional - Derivative (PD), b)Sliding Mode (SM) and c) PD+SM. The results of these control laws simulation are shown, respectively, in Figs. 5-7.

Note that the quadrotor aircraft reached the desired altitude using sliding mode control and PD control with Sliding Mode Compensation (PD+SM) while with only a PD control the error increase due to disturbances. Fig. 8 shows that PD+SM control presents the best performance since the error converges to zero, as in SM control, in a fast way.

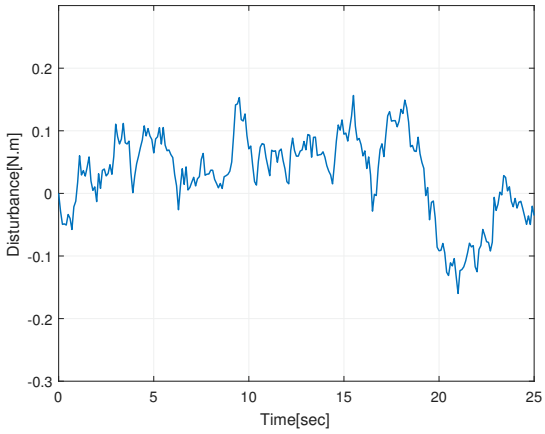

Fig. 4. Disturbance simulation from Dryden wind-gust model.

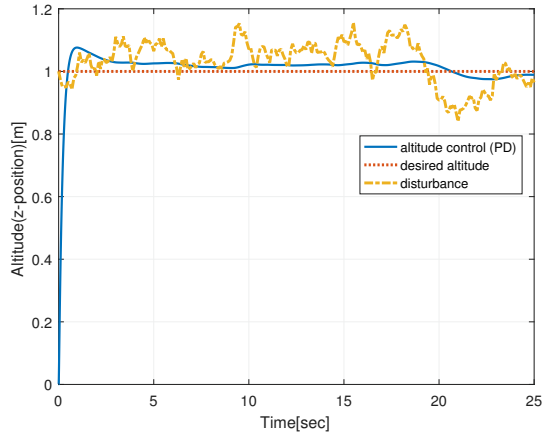

Fig. 5. Altitude PD control.

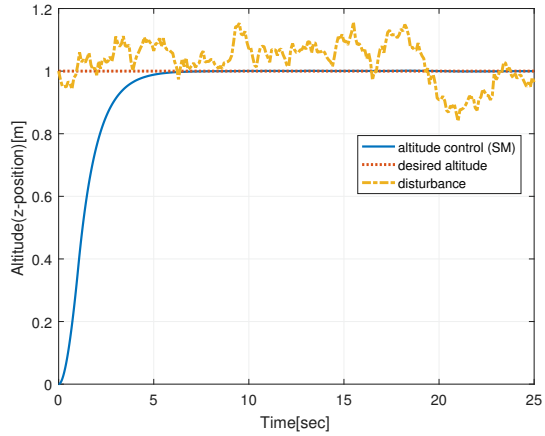

Fig. 6. Altitude sliding mode (SM) control.

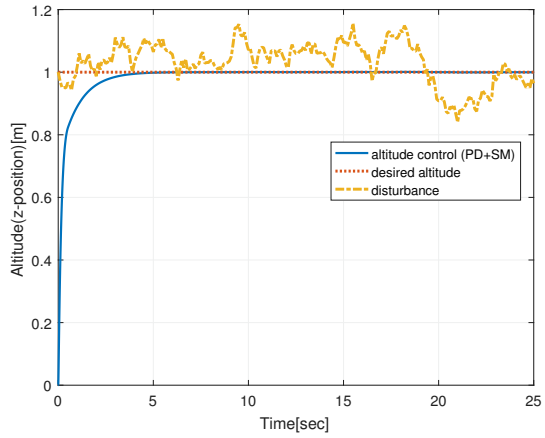

Fig. 7. Altitude PD+SM control.

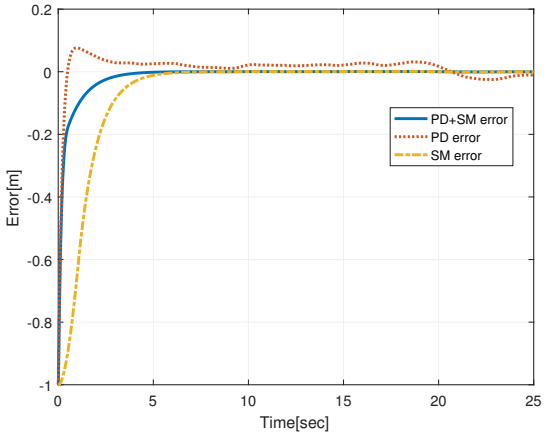

Fig. 8. Error comparison.

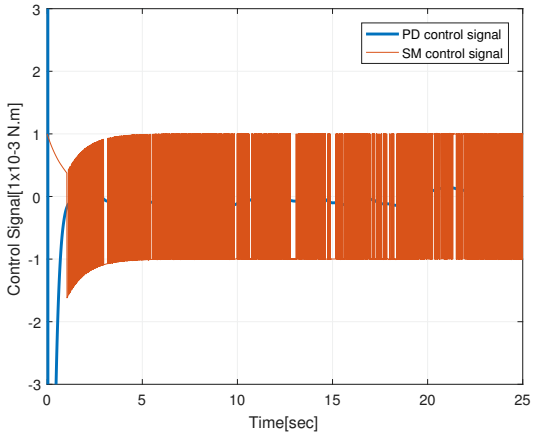

Fig. 9. Error comparison.

On the other hand, Fig. 9 shows the PD and SM control signals from simulation. Fig. 10 is a zoom from 9 to observe in a better way the signals.

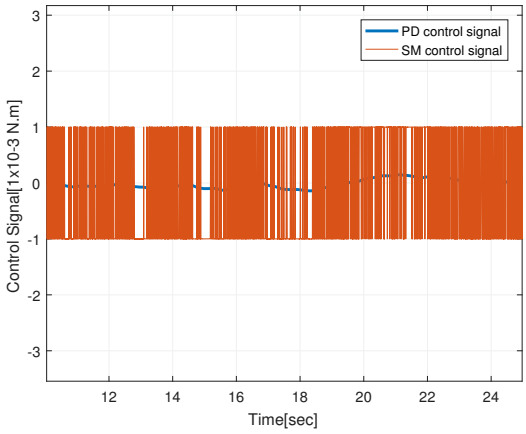

Fig. 10. Zoom from Fig. 9.

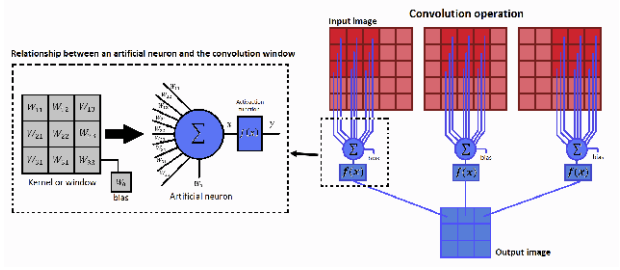

Fig. 11. Relationship between convolution window and a neuron.

6. CONVOLUTIONAL NEURONAL NETWORKS

In this work, a deep learning model called convolutional neuronal network (CNN) is used to determine if there exist cracks in images of buildings. The CNNs has been used to solve, in an effective way, different problems related to artificial vision (mainly related to the image recognition) and currently is an important research topic.

Classical algorithms for object detection are based on two-stage: features extraction and classification. By contrast, the CNNs implement this two-stage in the same process.

Fig. 11 shows the basic idea behind the CNN. In classical artificial neural networks, the synaptic weights (W_{ij}) and the bias W_0 determine the output of the network. On the other hand, in a CNN, a neuron and convolution window are equivalent. The parameters of the network (synaptic weights and bias) are the coefficients of the convolution window.

The convolution operation is performed sliding the the window (neuron) over the complete image. This convolution generate feature maps that represent the output of each layer of the network. The output y of one layer of the network is

$$y = Relu(\langle W, x \rangle + b), \tag{35}$$

where $\langle \cdot, \cdot \rangle$ represents the dot product between the tensor formed by the synaptic weights and x is the image on which the convolution operation is performed, b is a polarization value or bias while $Relu$ is the activation function.

At first, the synaptic weights W_{ij} are selected randomly and the training process modify them in such a way that the CNN is able to classify the cracks in the images.

The last stage within the network is dense or strongly connected, where the flow of information from the convolutional layers is connected to a conventional neural network that functions as a classifier. Since it is a bi-class problem, the last layer consists of a single neuron that will indicate whether or not there is a crack in the image.

In a CNN, the convolutional layers extracts features of the images to later be classified by a classical neural network.

7. EXPERIMENTAL RESULTS

This section describes the CNN which has been adopted for classifying cracks in images taken by a quadrotor, it is compared with a Viola-Jones classifier commonly used for this task. Also, our quadrotor aircraft platform is described briefly and real-time experimental results are shown. Several experiments were carried out to stabilize the altitude of our platform. The controller's parameters were tuned by trial and error until obtaining better performance.

7.1. Convolutional Neural Network Clasification

In order to perform the process of training the CNN and a Viola-Jones classifier, images of cracks were searched on the Internet, mainly of the earthquake in Mexico City in 2017. Fig. 12 shows some of the images from the database.

It is necessary to create two sets, the positive set, that is, those that contain cracks and the other of negatives, which do not contain cracks. We obtained 350 positive images and 450 negative images for a total of 800 images. All of them were resized to 50x50 pixels. In search of improving the detection results, our database was combined with the one used in [20], in such a way that the number of positive images was increased to 450.

Fig. 12. Samples of images with cracks taken from the Internet.

The developed network consists of four convolutional layers and two dense layers, as well as polling operations after each convolutional layer, as can be seen in Fig. 13. We use Keras [36] to create a CNN. Keras is a high-level neural networks API, written in Python and capable of running on top of TensorFlow, CNTK, or Theano [37]. We use a computer with AMD A8 processor and 8Gb of RAM to carry out the training stage, under the Ubuntu OS. A total of 400 positive and 400 negative images were used for training while for validation, 50 positive and 50 negative examples were used. A CNN obtained 95% accuracy in the training stage and 96% in the validation stage.

To implement the detection stage, a sliding window method was used. This method uses a fixed size window and this goes through the entire image in search of cracks.

Fig. 14a and 14c shows results from the detection using CNN. In general, the detection is satisfactory, with an acceptable amount of cracks detected and some false positives.

On the other hand, results from Viola-Jones classifier are shown in Fig. 14b and 14d. Even though detections are effective with this method, some false positives (red ellipses) detect as cracks the wall corner, which does not happen with CNN, in other words, our CNN can distinguish cracks from other edges in an acceptable way and the results are better than classical Viola-Jones classifier, as shown Fig. 15.

7.2. Quadorotor UAV real-time altitude control

As an experimental platform, we have used a quadrotor aircraft with a Pixhawk flight controller and a LIDAR-Lite v3 sensor for the altitude measure. This sensor was selected because it offers a better performance than the barometer. Fig. 16 shows the real-time embedded control architecture that we use. As is well known, the chattering problem (which is due to failures in switching devices and delays) is one of the most common handicaps in the sliding mode control. To reduce the chattering, we use the approach presented in [28] and replace the *sign* function, that is not continuous, for a continuous saturation function *sat*, defined as follows:

$$sat\left(\frac{s}{\varepsilon}\right) = \begin{cases} \dfrac{s}{|s|}, & |s| \geq \varepsilon, \\ \dfrac{s}{\varepsilon}, & |s| < \varepsilon, \end{cases} \tag{36}$$

where ε is a small positive constant. Fig. 17 present some experimental results obtained by applying the PD+SMC control algorithm. The arrows in Fig. 17b and 17d show the time interval where the SMC action was canceled, which correspond with the vertical dotted line in Fig. 17a and 17c. It is evident that the performance with PD+SMC is better than when the PD is working alone. Control gains

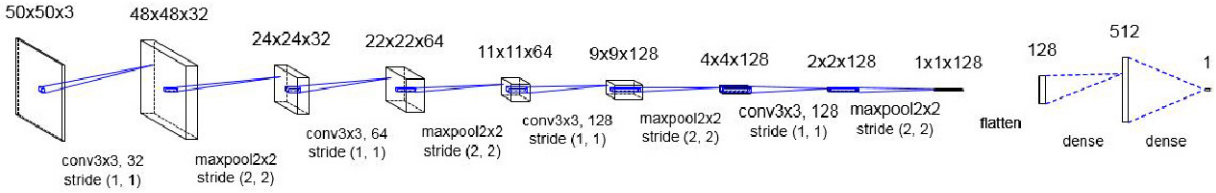

Fig. 13. Architecture of the proposed network.

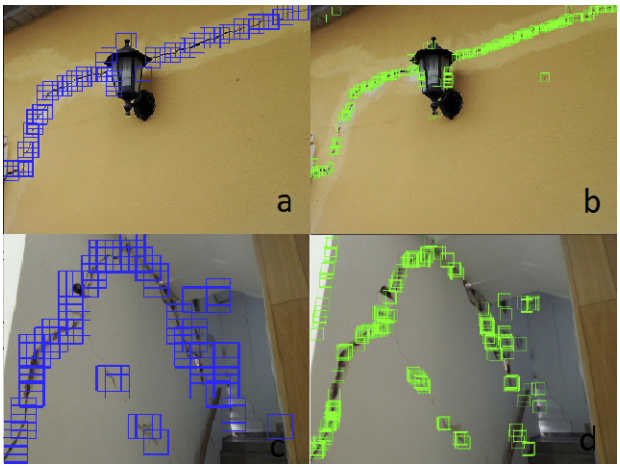

Fig. 14. Crack detection on the original images.

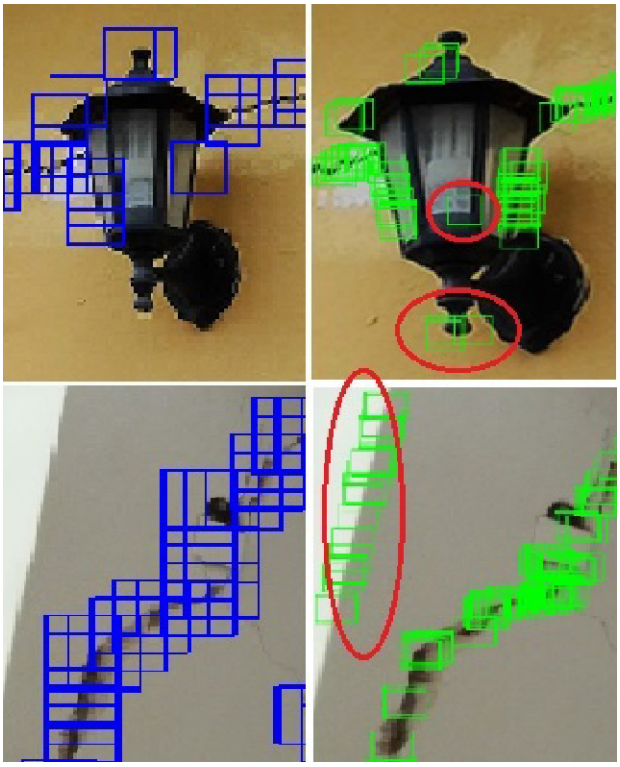

Fig. 15. Zoom from Fig. 14.

selection is a complicated task, and we made it by trial

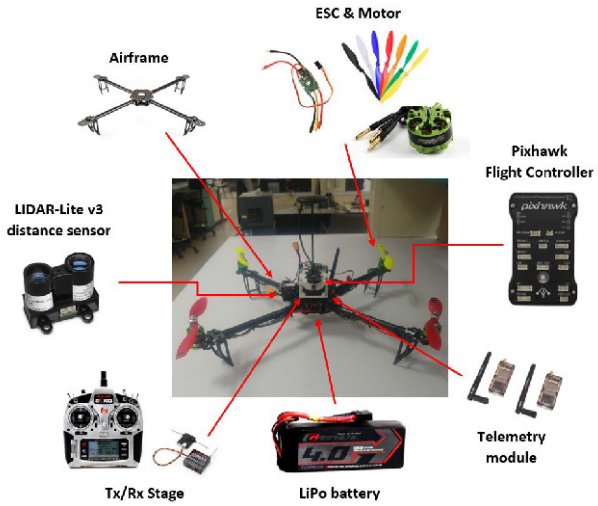

Fig. 16. Real-time embedded control architecture.

and error until obtaining the desired behavior. A properly k_p and k_d selection for a PD controller affects the performance of a control system, for instance, improving damping, reducing maximum overshoot, and reducing rise time and settling time. On the other hand, parameters λ and ρ in the SMC let modify the convergence velocity and sliding surface frequency, respectively. This results could be improved by fine-tuning ρ, λ, k_p and k_d gains. Fig. 18 show some experiments carried out at CINVESTAV.

8. CONCLUSIONS

The paper presents simulations and experimental real-time results in the altitude control using a combination of two control actions, one linear (PD) and another non-linear (Sliding Mode Control) for the future autonomous wall inspection task. The PD+SMC takes the advantages of the PD controller (simplicity and easy design) and the robustness of SMC to disturbances and model uncertainty. To our knowledge no works concerinig hybrid PD+SMC for UAV systems have been reported in literature. The simulations were conducted using the quadrotor aircraft dynamical model and the real-time experiments were performed in an outdoor environment where wind-disturbances were present. To see the flight that was carried out to test the control, a video is available on

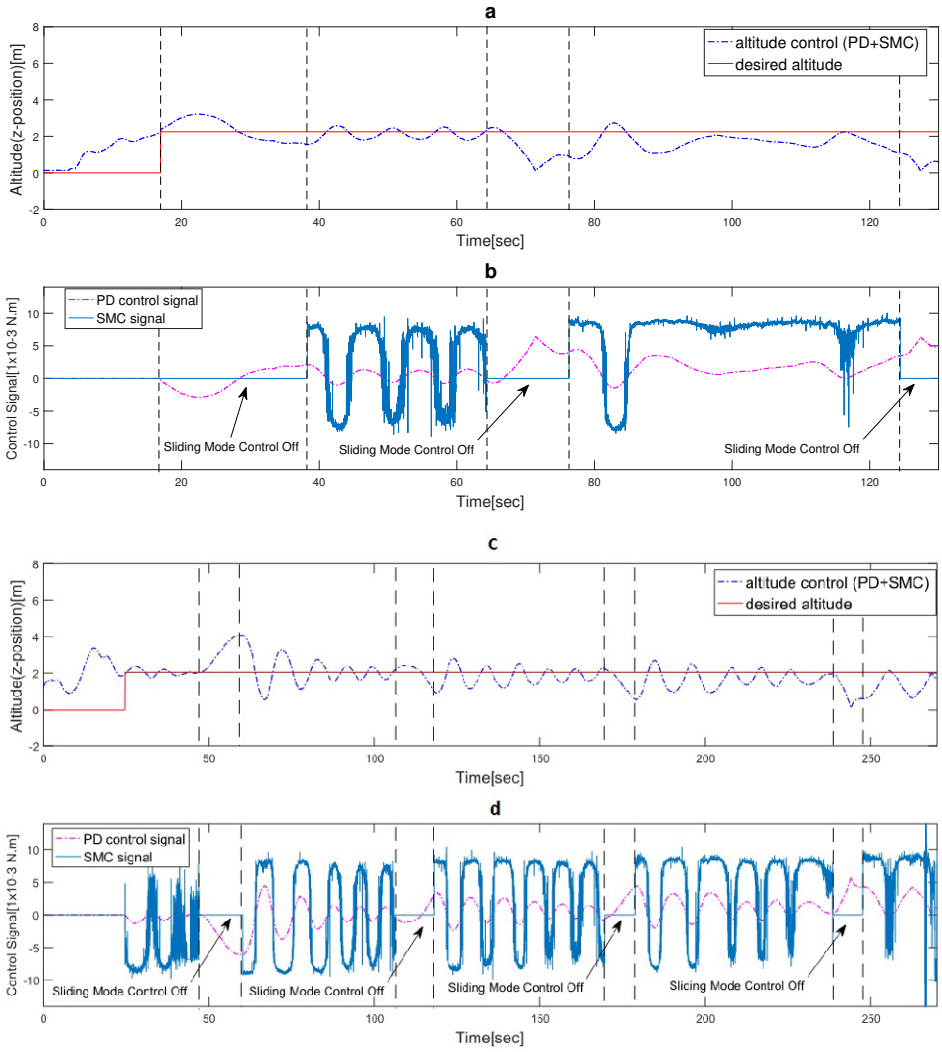

Fig. 17. Altitude position in real-time experiments.

Fig. 18. Quadrotor aircraft flight using PD+SMC for altitude control.

`https://youtu.be/Aph-DgsFRF8`. On the other hand, we increase our database of crack images for a CNN-based crack recognition system. The experiments showed that the recognition of the cracks is satisfactory. There are very few databases of images with cracks; it is important to have a greater number of images to be able to develop better applications of automatic detection of this type of anomalies. Generally, CNN has shown good results in object recognition tasks given their ability to train feature extractors and their classification stage.

REFERENCES

[1] J. M. Vazquez-Nicolas, E. Zamora, I. Gonzalez-Hernandez, R. Lozano, and H. Sossa, "Towards automatic inspection: crack recognition based on Quadrotor UAV-taken images," *Proc. of the International Conference on Unmanned Aircraft Systems (ICUAS)*, pp. 654-659, 2018.

[2] A. P. Sandiwan, A. Cahyadi, and S. Herdjunanto, "Robust proportional-derivative control on SO(3) with disturbance compensation for quadrotor UAV," *International Journal of Control, Automation and Systems*, vol. 15, no. 5, pp. 2329-2342, October 2017.

[3] H. Liu, Y. Bai, G. Lu, Z Shi, and Y. Zhong, "Robust tracking control of a quadrotor helicopter," *Journal of Intelligent & Robotic Systems*, vol. 75, no. 3-4, pp. 595-608, September 2014.

[4] M. Elfeky, M. Elshafei, A. A. Saif, and M. F. Al-Malki, "Modeling and simulation of quadrotor UAV with tilting rotors," *International Journal of Control, Automation and Systems*, vol. 14, no. 4, pp. 1047-1055, August 2016.

[5] R. Rafifandi, D. L. Asri, E. Ekawati, and E. M. Budi, "Leader-follower formation control of two quadrotor UAVs," *SN Applied Sciences*, vol. 1, no. 6, pp. 539, June 2019.

[6] S. Jeong and S. Jung, "Cartesian space control of a quadrotor system based on low cost localization under a vision system," *International Journal of Control, Automation and Systems*, vol. 14, no. 2, pp. 549-559, April 2016.

[7] Z. Zuo, "Trajectory tracking control design with command-filtered compensation for a quadrotor," *IET Control Theory & Applications*, vol. 4, no. 11, pp. 2343-2355, November 2010.

[8] S. Barghandan, M. A. Badamchizadeh, and M. R. Jahed-Motlagh, "Improved adaptive fuzzy sliding mode controller for robust fault tolerance of a quadrotor," *International Journal of Control, Automation and Systems*, vol. 15, no. 1, pp. 427-41, February 2017.

[9] R. López-Gutiérrez, A.E. Rodriguez-Mata, and S. Salazar, "Robust quadrotor control: attitude and altitude real-time results," *Journal of Intelligent & Robotic Systems*, vol. 88, no. 2-4, pp. 299-312, December 2017.

[10] A. Aboudonia, R. Rashad, and A. El-Badawy, "Composite hierarchical anti-disturbance control of a quadrotor UAV in the presence of matched and mismatched disturbances," *Journal of Intelligent & Robotic Systems*, vol. 90, no. 1-2, pp. 201-216, May 2018.

[11] J. Escareño, S. Salazar, and H. Romero, "Trajectory control of a quadrotor subject to 2d wind disturbances," *Journal of Intelligent & Robotic Systems*, vol. 70, no. 1-4, pp. 51-63, April 2013.

[12] Z. Liu, X. Liu, J. Chen, and C. Fang, "Altitude control for variable load quadrotor via learning rate based robust sliding mode controller," *IEEE Access*, vol. 7, pp. 9736-9744, January 2019.

[13] A. L'Afflitto, R. B. Anderson, and K. Mohammadi, "An introduction to nonlinear robust control for unmanned quadrotor aircraft: how to design control algorithms for quadrotors using sliding mode control and adaptive control techniques [Focus on Education]," *IEEE Control Systems Magazine*, vol. 38, no. 3, pp. 102-121, June 2018.

[14] L. R. Salinas, D. Santiago, E. Slawiñski, V. A. Mut, D. Chavez, P. Leica, and O. Camacho, "P+d plus sliding mode control for bilateral teleoperation of a mobile robot," *International Journal of Control, Automation and Systems*, vol. 16, no. 4, pp. 1927-1937, August 2018.

[15] P. R. Ouyang, J. Acob, and V. Pano, "PD with sliding mode control for trajectory tracking of robotic system," *Robotics and Computer-Integrated Manufacturing*, vol. 30, no. 2, pp. 189-200, April 2014.

[16] J. Tang, P. R. Ouyang, W. H. Yue, and H. M. Kang, "Nonlinear PD sliding mode control for robotic manipulator," *Proc. of the IEEE International Conference on Advanced Intelligent Mechatronics (AIM)*, pp. 1004-1008, 2017.

[17] P. R. Ouyang, J. Tang, W. H. Yue, and S. Jayasinghe, "Adaptive PD plus sliding mode control for robotic manipulator," *Proc. of the IEEE International Conference on Advanced Intelligent Mechatronics (AIM)*, pp. 930-934, 2016.

[18] Newspaper "La Razon", "Damaged building in the earthquake in Mexico City," La Razon, 12 July, 2018, www.razon.com.mx/, Accessed: September 1, 2018.

[19] R. G. Lins and S. N. Givigi, "Automatic crack detection and measurement based on image analysis," *IEEE Transactions on Instrumentation and Measurement*, vol. 65, no. 3, pp. 583-590, March 2016.

[20] Y. Shi, L. Cui, Z. Qi, F. Meng, and Z. Chen, "Automatic road crack detection using random structured forests," *IEEE Transactions on Intelligent Transportation Systems*, vol. 17, no. 12, pp. 3434-3445, Decemeber 2016.

[21] A. M. A. Talab, Z. Huang, F. Xi, and L. HaiMing, "Detection crack in image using Otsu method and multiple filtering in image processing techniques," *Optik*, vol. 127, no. 3, pp. 1030-1033, February 2016.

[22] M. D. Phung, V. T. Hoang, T. H. Dinh, and Q. Ha, "Automatic crack detection in built infrastructure using unmanned aerial vehicles," *Proc. of the 34th International Symposium on Automation and Robotics in Construction*, pp. 823-829, 2017.

[23] L. Wang and Z. Zhang, "Automatic detection of wind turbine blade surface cracks based on UAV-taken images," *IEEE Transactions on Industrial Electronics*, vol. 64, no. 9, pp. 7293-7303, Septemeber 2017.

[24] S. S. Choi and E. K. Kim, "Building crack inspection using small UAV," *Proc. of the 17th International Conference on Advanced Communication Technology (ICACT)*, pp. 235-238, 2015.

[25] N. Sun, T. Yang, Y. Fang, Y. Wu, and H. Chen, "Transportation control of double-pendulum cranes with a nonlinear quasi-PID scheme: design and experiments," *IEEE Transactions on Systems, Man, and Cybernetics: Systems*, vol. 49, no. 7, pp. 1408-1418, July 2019.

[26] R. Lozano, *Unmanned Aerial Vehicles: Embedded Control*, Wiley, Hoboken, NJ, 2013.

[27] P. Castillo, A. Dzul, and R. Lozano, "Real-time stabilization and tracking of a four-rotor mini rotorcraft," *IEEE Transactions on Control Systems Technology* , vol. 12, no. 4, pp. 510-516, July 2004.

[28] I. Gonzalez, S. Salazar, and R. Lozano, "Chattering-free sliding mode altitude control for a quad-rotor aircraft: real-time application," *Journal of Intelligent & Robotic Systems*, vol. 73, no. 1-4, pp.137-155, January 2014.

[29] L. Yang, B. Li, W. Li, Z. Liu, G. Yang, and J. Xiao,"Deep concrete inspection using unmanned aerial vehicle towards CSSC database," *Proc. of the IEEE/RSJ International Conference on Intelligent Robots and Systems (IROS)*, 2017.

[30] C. Pan, X. Cao, and D. Wu, "Power line detection via background noise removal," *Proc. of the IEEE Global Conference on Signal and Information Processing (GlobalSIP)*, pp. 871-875, 2016.

[31] T. Tang, Z. Deng, S. Zhou, L. Lei, and H. Zou, "Fast vehicle detection in UAV images," *Proc. of the International Workshop on Remote Sensing with Intelligent Processing (RSIP)*, pp. 1-5, 2017.

[32] J. S. Zhang, J. Cao, and B. Mao, "Application of deep learning and unmanned aerial vehicle technology in traffic flow monitoring," *Proc. of the International Conference on Machine Learning and Cybernetics (ICMLC)*, pp. 189-194, 2017.

[33] Y. Ma, Y. Liu, R. Jin, X. Yuan, R. Sekha, S. Wilson, and R. Vaidyanathan, "Hand gesture recognition with convolutional neural networks for the multimodal UAV control," *Proc. of the Workshop on Research, Education and Development of Unmanned Aerial Systems (RED-UAS)*, pp. 198-203, 2017.

[34] L. Zhang, F. Yang, Y. Daniel Zhang, and Y. J. Zhu, "Road crack detection using deep convolutional neural network," *Proc. of the IEEE International Conference on Image Processing (ICIP)*, pp. 3708-3712, 2016.

[35] H. K. Khalil, *Nonlinear Control*, pp. 244, Pearson, 2014.

[36] F. Chollet, *Keras*, 2015, GitHub, https://github.com/keras-team/keras, Accessed: September 29, 2018.

[37] F. Chollet, *Keras: The Python Deep Learning library*, https://github.com/keras-team/keras, Accessed: September 29, 2018.

J. M. Vázquez-Nicolás was born in Mexico City, on January 6, 1990. He received his B.S. degree in Mechatronics and M.S. in Computer Engineering from National Polytechnic Institute of Mexico, in 2013 and 2016, respectively. He is currently working toward a Ph.D. degree at CINVESTAV-IPN. His current research interests include the area of dynamics and control of UAV, artificial intelligence and robotics systems.

Erik Zamora is a full professor with the National Polytechnic Institute of Mexico. He received his Diploma in Electronics from UV (2004), his Master's degree in Electrical Engineering from CINVESTAV (2007), and his PhD in automatic control from CINVESTAV (2015). He developed the first commercial Mexican myoelectric system to control a prosthesis in the Pro/Bionics company and a robotic navigation system for unknown environments guided by emergency signals at the University of Bristol. He had a postdoctoral position in CIC-IPN for two years (2016-2017). His current interests include autonomous robots and machine learning. He has published 18 technical papers in international conference proceedings and journals and has directed 19 theses on these topics.

Iván González-Hernández was born in Mexico City, on March 18, 1981. He received an engineering degree in Communications and Electronics from the Instituto Politécnico Nacional, Mexico City, in 2003, and his M.Sc. and Ph.D. studies in Automatic Control at the Centro de Investigación y de Estudios Avanzados (CINVESTAV), Mexico City, in 2009 and 2013, respectively. At present, he works as research professor in the UMI-LAFMIA 3175 CNRS laboratory by agreement called Catédra-CONACYT, where his current research interests include real-time robust control applications, sliding mode control techniques and embedded control systems in Unmanned Aerial Vehicles (UAV) in particular the Quad-rotor aircraft configuration.

Rogelio Lozano was born in Monterrey Mexico, on July 12, 1954. He received his B.S. degree in Electronic Engineering from the National Polytechnic Institute (IPN) of Mexico in 1975, an M.S. degree in Electrical Engineering from CINVESTAV-IPN, Mexico in 1977, and a Ph.D. degree in Automatic Control from LAG, INPG, France, in 1981. He joined the Department of Electrical Engineering at the CINVESTAV, Mexico, in 1981 where he worked until 1989 and is a CNRS Research Director since 1990. Since April 2008 he is the head of the UMI 3175 LAFMIA at CINVESTAV Mexico, which is a joint research laboratory founded by CNRS, CINVESTAV and CONACYT. He is author or co-author of 86 journal papers, 164 conference presentations and 5 Springer-Verlag books in the areas of control and observers for non linear dynamical systems, adaptive control, passive systems, modeling and control of small UAV and localization of UAV using vision systems or radio signals.

Humberto Sossa was born in Guadalajara, Jalisco, Mexico in 1956. He received his B.Sc. degree in Electronics from the University of Guadalajara in 1981, an M.Sc. degree in Electrical Engineering from CINVESTAV-IPN in 1987, and a Ph.D. degree in Informatics from the National Polytechnic Institute of Grenoble, France in 1992. He is a full time professor at the Centre for Computing Research of the National Polytechnic Institute of Mexico. He is also the Head of the Robotics and Mechatronics Laboratory. His main research interests are in Artificial Intelligence, Machine Learning and Robotics.

Publisher's Note Springer Nature remains neutral with regard to jurisdictional claims in published maps and institutional affiliations.